Mn^{2+}-, Fe^{2+}-, Co^{2+}-, Ni^{2+}-, Cu^{2+}-, and Zn^{2+}-Binding Chalcogen−Chalcogen Bridges: A Compared MP2 and B3LYP Study

Yannick Jeanvoine and Riccardo Spezia*

Laboratoire Analyse et Modélisation pour la Biologie et l'Environnement, UMR 8587 CNRS, Université d'Evry Val d'Essonne, Bd F. Mitterrand, 91025 Evry Cedex, France

Received: December 29, 2008; Revised Manuscript Received: May 4, 2009

We investigated the binding of late first row transition metals with chalcogen−chalcogen bridges represented by minimal models (H_2O_2, H_2S_2, and H_2Se_2). The use of such small models allows us to employ a large atomic basis set and compare DFT and MP2 results with CCSD(T) reference data. All methods agree in finding Cu^{2+} complexes the most stable ones, and for each given metal, H_2Se_2 complexes are more stable than H_2S_2 ones and the latter more stable than the corresponding H_2O_2 ones. Despite this qualitative agreement between all the considered methods, quantitatively we found a big difference between MP2 and B3LYP, in structural and energetic properties. In particular, DFT largely overestimates the binding energies, while MP2 slightly underestimates them with respect to CCSD(T) calculations. Note that also other popular functionals (MPW1PW91, M05, TPSS, BLYP, and SVWN) overestimate the binding energy, such that it seems to be an intrinsic DFT failure. The main discrepancy was found for Cu^{2+}. The comparative analysis of B3LYP and MP2 wave functions explains the differences found between two methods and why the Cu^{2+} complexes show the bigger one. Finally, CCSD(T) calculations, slightly modifying MP2 insights, found that all three complexes present the same metal binding energy order, and notably $Cu^{2+} > Ni^{2+} > Zn^{2+} > Co^{2+} > Fe^{2+} > Mn^{2+}$.

1. Introduction

Transition metals often play a crucial role in biological systems, where they are always present in the cationic form, binding many different biological molecules.[1] In general, transition metal binding is a key process involved in several fields, e.g., catalysis, organometallic reactions, biological regulation, and environmental toxicology. Thus, fundamental investigations on metal binding to molecules being simple models of complex biological chelators, often called biomimetic molecules, have become the subject of several theoretical and experimental studies in the past few years.[2−9] Some first row transition metals (like Mn, Fe, Ni, Cu, Zn) are essential for organisms at a low level; others are present as rare elements (like Co present only in vitamin B12). While they have a biological role at low concentrations, they become toxic at high concentrations and their toxicity is still the subject of extensive research.[10,11] In particular, since they are mostly present at the same oxidation state (II), a metal that becomes too abundant, generally as a result of an external contamination of the organism, can take the place of another transition metal, thus modifying the biochemical cycles in which the physiological metal is involved and/or its structural function. Some of them (Mn, Fe, Cu) can have different oxidation states in the biological environment, and thus, they can be involved in redox regulation in biological (and, more generally, in catalytic) processes.[12−14] The systematic study of a whole chemical series is a preferential way to rationalize and thus understand chemical bonding and molecule−metal interactions.[15−19]

Among biological systems, proteins and polypeptides are the main targets for metal binding. The most relevant amino acids able to bind metal cations are the side chains of histidine, cysteine, aspartic acid, and glutamic acid. Cysteine is the only naturally occurring thiol-containing amino acid, giving its unique and fundamental properties in structure and activity of biomolecules. In particular, it is recognized that the coordination of metal cations can be achieved through sulfur sites in a variety of proteins and metalloenzymes.[20−23] Cysteine side chains can be directly involved in redox processes, and they have the unique characteristic of being able to form S−S bridges that can link amino acids that are not adjacent in the peptide or protein chain. These bridges are fundamental for structure stability, and their making and breaking, corresponding to redox reactions of thiolate groups, can be involved in metal binding processes.[24] Sulfur of cysteine can be replaced by selenium, the chalcogen element located just below sulfur in the periodic table, forming selenocysteine. Proteins where Se substitutes S play a variety of important roles in cellular activity.[25−29] While the functions of selenoproteins are not always certain, one role may concern chelation of heavy metals.[26] In some cases selenium seems to have an important role in protection against metal toxicity.[30,31] These findings could suggest a specificity of Se in binding metals, but the microscopic basis of this behavior is still unknown. In recent work, we investigated binding of Co(II) to cysteine and selenocysteine, where the chalcogen is both protonated and deprotonated, but we did not find any large difference in binding.[32] We suggested that differences may come from the interaction with S−S and Se−Se bridges that can be formed during the chelation process. To this end, in the present study, we performed a systematic investigation of the binding of late first row transition metals at the same oxidation state (II) with chalcogen bridges. For the sake of completeness, we also studied the binding with O−O bridges in order to understand the properties along group VIa. To use large basis sets in DFT, MP2, and CCSD(T) calculations we considered the smaller model systems for chalcogen−chalcogen bridges,

* To whom correspondence should be addressed. Phone: +33-1-69 47 76 53. Fax: +33-1-69 47 76 55. E-mail: riccardo.spezia@univ-evry.fr.

10.1021/jp811460f CCC: $40.75 © 2009 American Chemical Society
Published on Web 06/12/2009

i.e., H_2O_2, H_2S_2, and H_2Se_2. DFT with the popular B3LYP hybrid functional[33] is nowadays the most common quantum chemistry method computationally available for relatively large systems, but even if it can provide good results in many cases,[34−36] it can often fail, especially when treating transition metals,[37−44] such that recently a great amount of theoretical development was devoted to building new functionals.[45,46] In particular, DFT can produce severe errors due to the difficulty in treating the static (or nondynamical) correlation effects.[39,41] Thus, a comparison between different theoretical methods is fundamental, since it can provide a guide for interpreting results that can be obtained only at one theoretical level. At this end, we investigated the performance of different types of DFT approaches classified in terms of the kind of functionals they employ: (i) the local spin density approximation (LSDA), (ii) the generalized gradient approximation (GGA), (iii) hybrid DFT functionals combining GGAs with Hartree−Fock exchange (B3LYP stays in this class), (iv) meta-GGA functionals, and (v) hybrid-meta-GGA combining GGAs, meta functionals, and Hartree−Fock exchange. Furthermore, both MP2 and DFT methods must be related to experimental or more accurate theoretical calculations, like coupled-cluster or multiconfigurational methods, in order to identify which is the better performing method. In the present work, since a set of small systems was considered and no experimental data are available to the best of our knowledge, we compared MP2 and DFT results with CCSD(T) ones, thus providing a guide for the use of both methods for larger systems.

The outline of the remainder of the text is as follows. In section 2 we describe the methods employed to solve electronic structure problems and to obtain different properties. In section 3.1 we show results on the structural properties, then in section 3.2 we focus on the binding energy properties, and in section 3.3 we present the wave function analysis using population analysis providing us with information on electron localization and binding properties. In section 4 we summarize and give conclusions.

2. Theoretical Calculations

Geometry optimizations and frequency calculations were performed using density functional theory (DFT) with different functionals and using Moeller−Plesset perturbation theory at second order (MP2).

The retained functionals were the following:B3LYP, a very popular hybrid-GGA functional[33] used in several recent studies on transition metals binding to biomimetic and biological molecules;[47−49] MPW1PW91, another commonly used hybrid functional;[50] M05, a new hybrid-meta-GGA functional;[51] TPSS, a meta-DFT functional with TPSS exchange and TPSS correlation (also called TPSSTPSS);[52] BLYP, a GGA functional with Becke88 exchange[53] and Lee−Yang−Parr correlation;[54,55] SVWN, the well-known local spin density approximation (LSDA) with the Slater exchange[56] and the VWN correlation functional.[57]

The following basis set was used in both DFT and MP2 calculations: a 6-311++G(2df,2p) basis for O, S, Se, and H atoms and a 6-311+G(2d,2p) basis for first row transition metals. The use of these two different basis sets are a good agreement between computational costs and results reliability as pointed out by recent studies.[32,58−60]

For all the systems having more than one possible spin state, we performed calculations for all possible states finding that the following spin states are most stable across the transition metal series: sextet for Mn(II), quintet for Fe(II), quartet for Co(II), triplet for Ni(II), and doublet for Co(II). These open-shell systems were studied using the unrestricted formalism. Zn(II) is the only singlet state, and the restricted formalism was employed. In this study we report only results for those most stable spin states. The possibility of spin contamination was carefully checked in all results, finding a very small wave function contamination ($\langle S^2\rangle_{\text{calculated}} - \langle S^2\rangle_{\text{exact}} < 0.026$). Basis set superposition error (BSSE) was estimated using the counterpoise method of Boys and Bernardi.[61] This effect was found to be less than 1 kcal/mol for the B3LYP method and less than 3 kcal/mol for the MP2 method. The stability of the wave function was also tested for each SCF calculation, and the wave function was eventually reoptimized if an instability was detected.

Thermochemistry was investigated by standard thermochemical analysis performed on the minimum energy structure in the harmonic approximation using standard expressions for an ideal gas in the canonical ensemble.[62] For all the reported structures, zero-point energy (ZPE) was added from vibrational analysis. Net atomic charges have been obtained using the natural population analysis of Weinhold and co-workers.[63,64]

MP convergence was checked by doing single-point perturbation calculations up to the fourth order from the geometries optimized at the MP2 level. CCSD(T) single-point calculations were also conducted on both MP2- and B3LYP-optimized structures.

All of the above calculations were performed with the Gaussian03 package.[65]

3. Results and Discussions

3.1. Structural Data. To understand the binding properties of transition metals (M) from Mn^{2+} to Zn^{2+} with H_2O_2, H_2S_2, and H_2Se_2, we first optimized at both the B3LYP and MP2 levels the unbound molecules, which can be characterized, from a structural point of view, by two distances, X−X (here and hereafter X stands for O, S, or Se) and XH, the HXX angle, and the dihedral angles HXXH. Further, the structure of each $(MH_2X_2)^{2+}$ complex was optimized with both B3LYP and MP2 methods. The three distances of each optimized complex (the same as the unbound one plus a metal−chalcogen distance MX) are reported in Table 1. In Table 2 we report angular optimized parameters. Note that we obtained symmetric structures (and the geometry optimization was performed without any symmetry constraint) such that we have identical MX distances and HXX angles. In the Supporting Information we report all the optimized molecular coordinates. The resulting structures are very similar for each complex: the metal bounds in the middle of the XX bond, such that both XM distances are identical, i.e., we have symmetric structures as expected (see Figure 1). As we can see from Table 2, the main binding difference between H_2O_2 and H_2S_2 or H_2Se_2 is the noticeable increase of the dihedral angle with respect the unbound H_2X_2 that is induced only for H_2S_2 and H_2Se_2 and not for H_2O_2, as also shown in Figure 1. To better show the binding behavior across the series, we report in Figures 2 and 3 XX and XM distances. As is clearly shown, upon binding the XX distance always increases, with the exception of Cu^{2+} binding H_2O_2 for B3LYP calculations and for both B3LYP and MP2 ones in the case of H_2S_2 and H_2Se_2. It is evident also from these structural results, and it will be more evident investigating binding energies and electronic structure, that there is a large difference in B3LYP and MP2 results in particular for Cu^{2+} binding: while MP2 reports a decrease in MX distances up to Cu and then a larger one for Zn, B3LYP finds that Cu−X distances are larger than those of both Ni and Zn complexes. B3LYP also provides a bigger

TABLE 1: Distances (in Å) Obtained from Geometry Optimizations at the B3LYP and MP2 Levels of Theory for the Different Complexes[a]

	d(X−X)		*d*(X−M)		*d*(X−H)	
	B3LYP	MP2	B3LYP	MP2	B3LYP	MP2
H_2O_2	1.4487	1.4481			0.9658	0.9640
$(MnH_2O_2)^{2+}$	1.4620	1.4678	2.1080	2.1355	0.9879	0.9844
$(FeH_2O_2)^{2+}$	1.4599	1.4704	2.0546	2.0678	0.9911	0.9867
$(CoH_2O_2)^{2+}$	1.4555	1.4729	2.0165	2.0176	0.9928	0.9880
$(NiH_2O_2)^{2+}$	1.4513	1.4768	1.9997	1.9786	0.9955	0.9893
$(CuH_2O_2)^{2+}$	1.4131	1.4747	2.0664	1.9347	1.0012	0.9922
$(ZnH_2O_2)^{2+}$	1.4886	1.4907	2.0169	1.9997	0.9909	0.9894
H_2S_2	2.0821	2.0636			1.3472	1.3386
$(MnH_2S_2)^{2+}$	2.1736	2.1546	2.4906	2.5136	1.3593	1.3516
$(FeH_2S_2)^{2+}$	2.1572	2.1565	2.4309	2.4145	1.3614	1.3529
$(CoH_2S_2)^{2+}$	2.1459	2.1559	2.3874	2.3630	1.3624	1.3538
$(NiH_2S_2)^{2+}$	2.1417	2.1609	2.3656	2.3059	1.3635	1.3550
$(CuH_2S_2)^{2+}$	2.1039	2.1151	2.4286	2.2186	1.3658	1.3579
$(ZnH_2S_2)^{2+}$	2.2581	2.2114	2.3743	2.3363	1.3614	1.3556
H_2Se_2	2.3578	2.3122			1.4742	1.4581
$(MnH_2Se_2)^{2+}$	2.4738	2.4301	2.6163	2.6357	1.4855	1.4694
$(FeH_2Se_2)^{2+}$	2.4530	2.4322	2.5565	2.5040	1.4875	1.4712
$(CoH_2Se_2)^{2+}$	2.4367	2.4304	2.5165	2.4815	1.4882	1.4716
$(NiH_2Se_2)^{2+}$	2.4342	2.4342	2.4891	2.4206	1.4892	1.4726
$(CuH_2Se_2)^{2+}$	2.3955	2.3711	2.5419	2.3171	1.4090	1.4747
$(ZnH_2Se_2)^{2+}$	2.5664	2.4957	2.4928	2.4464	1.4884	1.4739

[a] Unbound values are also reported. X = O, S, Se and M = Mn, Fe, Co, Ni, Cu, Zn.

TABLE 2: Angles (in degrees) Obtained from Geometry Optimizations at the B3LYP and MP2 Levels of Theory for the Different Complexes[a]

	a(HXX)		*a*(XMX)		di(HXXH)	
	B3LYP	MP2	B3LYP	MP2	B3LYP	MP2
H_2O_2	100.8	99.8			114.7	115.3
$(MnH_2O_2)^{2+}$	105.7	104.4	40.6	40.2	96.1	93.0
$(FeH_2O_2)^{2+}$	105.6	104.6	41.6	41.7	102.9	96.8
$(CoH_2O_2)^{2+}$	105.4	104.4	42.3	42.8	108.5	100.6
$(NiH_2O_2)^{2+}$	105.3	104.5	42.6	43.8	113.9	102.7
$(CuH_2O_2)^{2+}$	104.7	104.4	40.0	44.8	132.3	108.4
$(ZnH_2O_2)^{2+}$	105.4	104.1	43.3	43.8	100.1	100.7
H_2S_2	98.4	97.8			90.9	91.0
$(MnH_2S_2)^{2+}$	94.6	94.3	51.7	50.8	156.4	152.5
$(FeH_2S_2)^{2+}$	94.4	94.1	52.7	53.0	160.5	155.3
$(CoH_2S_2)^{2+}$	94.5	94.1	53.4	54.3	161.7	157.4
$(NiH_2S_2)^{2+}$	94.4	93.9	53.8	55.9	164.1	159.7
$(CuH_2S_2)^{2+}$	94.1	94.2	51.3	56.9	169.2	164.6
$(ZnH_2S_2)^{2+}$	93.6	93.0	56.8	56.5	160.6	161.7
H_2Se_2	96.6	96.3			90.4	90.6
$(MnH_2Se_2)^{2+}$	92.0	91.5	56.4	54.9	167.2	164.3
$(FeH_2Se_2)^{2+}$	92.0	91.5	57.3	58.1	168.5	165.4
$(CoH_2Se_2)^{2+}$	92.2	91.5	57.9	58.6	169.1	166.3
$(NiH_2Se_2)^{2+}$	92.1	91.5	58.5	60.4	170.5	167.7
$(CuH_2Se_2)^{2+}$	92.0	92.1	56.2	61.6	173.0	169.9
$(ZnH_2Se_2)^{2+}$	91.3	90.5	62.0	61.3	170.2	170.7

[a] Unbound values are also reported. X = O, S, Se and M = Mn, Fe, Co, Ni, Cu, Zn.

decrease in XX distances corresponding to the Cu^{2+} binding with respect to other metals, while MP2 finds a minimum that is not so pronounced and almost constant XX values for the other atoms in the series, except Zn^{2+}, which induces a clear increasing of this distance as reported from both methods. Also, the behavior of optimized angles across the series shows that B3LYP provides a "discontinuity" for Cu^{2+} that is not noticed by MP2 (see Table 2 and Figure 3).

As we will see, this discrepancy is even more evident from binding energy analysis, where we compared B3LYP and MP2 results with CCSD(T) ones, which can be considered as reference values, and with results obtained with other different popular functionals.

3.2. Binding Energies. Binding energy differences (ΔE) and free energies (ΔG) obtained at the B3LYP and MP2 level are reported in Tables 3 and 4, respectively. In the Supporting Information we report all other energetic data, i.e., ΔE + ZPE correction and enthalpy differences. We note that for each chalcogen the binding is stabilized moving from Mn^{2+} to Cu^{2+} and then Zn^{2+} has a binding energy similar to that of Ni^{2+}. This gap is larger passing from O to S and then to Se.

As it is evident from Tables 3 and 4, B3LYP provides for every complex a larger stabilization, in particular for Cu^{2+} complexes. Moving along the transition metal series, the Cu^{2+} complexes are the most stable for all the chalcogens, with an increasing stabilization with respect to other transition metal cations for S and Se. Thus, the Cu^{2+} complex with H_2O_2 is 48 kcal/mol more stable than the Mn^{2+} one while only 29 kcal/mol more stable as provided by MP2 calculations. Cu^{2+} forms complexes with H_2S_2 and H_2Se_2 much more stable than those with Mn^{2+}, 55−60 kcal/mol from MP2 calculations and 87−94 kcal/mol from B3LYP ones. Even though there is a qualitatively similar behavior across the series between B3LYP and MP2, differences in binding affinities are large, changing the binding affinity order as a function of the transition metal. MP2 provides for H_2O_2 the binding affinity order $Cu^{2+} > Ni^{2+} > Zn^{2+} > Co^{2+} > Fe^{2+} > Mn^{2+}$, while for H_2S_2 and H_2Se_2 the order is $Cu^{2+} > Zn^{2+} > Ni^{2+} > Co^{2+} > Fe^{2+} > Mn^{2+}$, where binding affinities of Ni^{2+} and Zn^{2+} are very similar for MP2 calculations. B3LYP, on the other hand, provides a different binding affinity order and the same for H_2O_2 and H_2S_2, notably $Cu^{2+} > Ni^{2+} > Co^{2+} > Zn^{2+} > Fe^{2+} > Mn^{2+}$, while for H_2Se_2 the order is $Cu^{2+} > Ni^{2+} > Zn^{2+} > Co^{2+} > Fe^{2+} > Mn^{2+}$. Note that B3LYP calculations provide a higher interaction energy for Co^{2+} since also in the case of H_2Se_2 the Zn^{2+} binding energy is only about 2 kcal/mol bigger than that of Co^{2+} and not similar to those of Ni^{2+} as reported by MP2 calculations. We should note that calculations done with B3LYP on Co(II) binding Cysteine and SeCysteine have found a difference in the gas-phase metal affinity of only 4.89 and 0.62 kcal/mol for neutral and deprotonated amino acids, respectively.[32] For the present

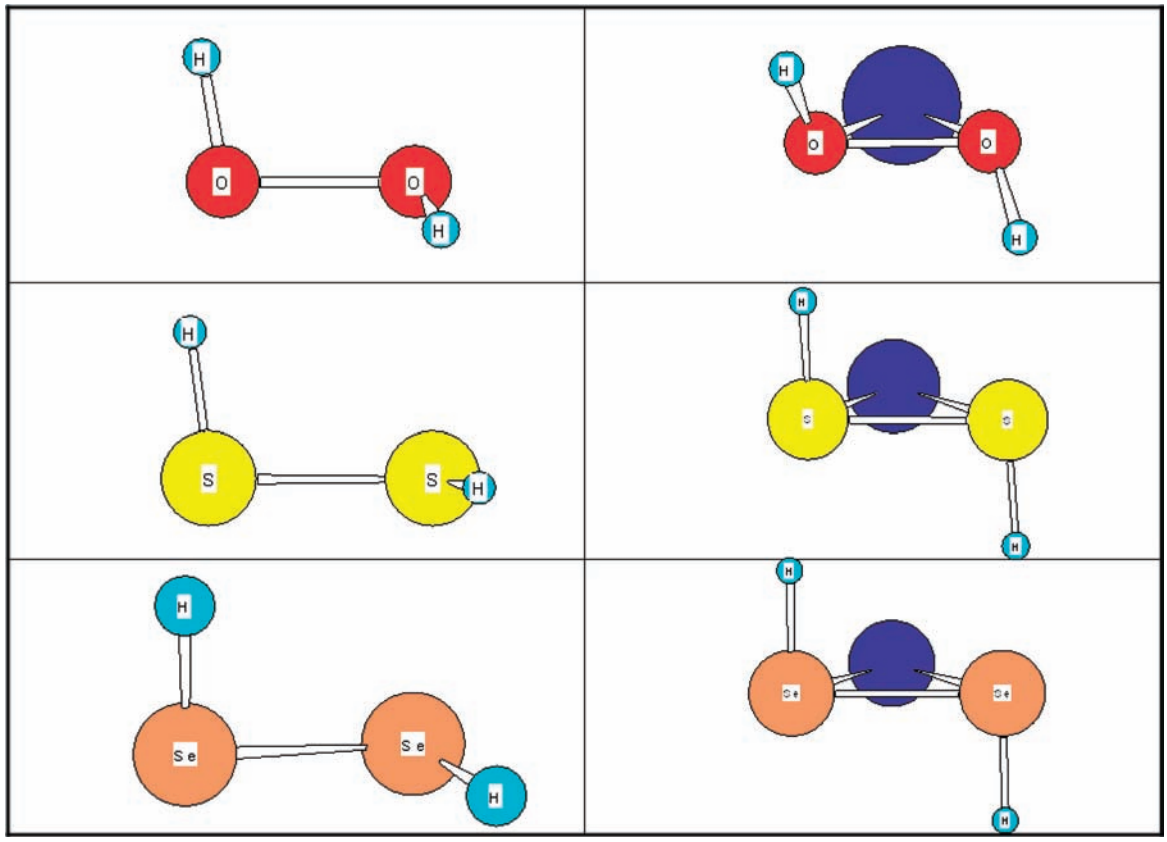

Figure 1. Unbound H_2O_2, H_2S_2, and H_2Se_2 structures (left column), and the same structures where a metal (blue) is bound.

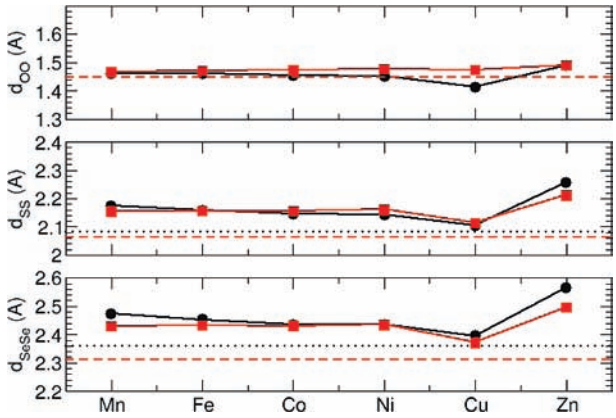

Figure 2. OO, SS, and SeSe distances obtained from B3LYP (circles) and MP2 (squares) calculations as a function of the binding metal. The unbound values are also reported (B3LYP (dotted) and MP2 (dashed)).

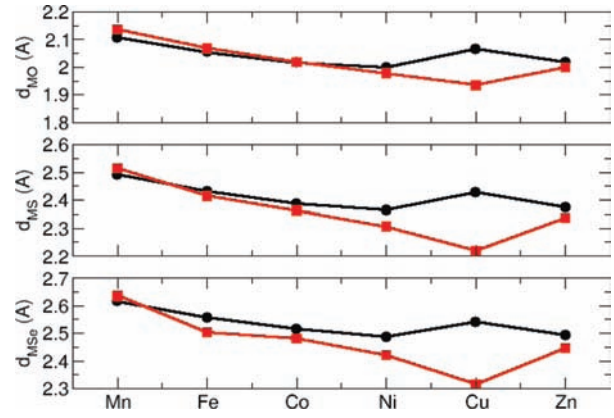

Figure 3. MO, MS, and MSe distances obtained from B3LYP (circles) and MP2 (squares) calculations as a function of the binding metal.

TABLE 3: Binding Energy (ΔE, in kcal/mol) Calculated at the B3LYP and MP2 Levels

	H_2O_2		H_2S_2		H_2Se_2	
	B3LYP	MP2	B3LYP	MP2	B3LYP	MP2
Mn^{2+}	–87.40	–78.77	–106.82	–89.73	–118.35	–97.86
Fe^{2+}	–99.57	–88.50	–127.80	–104.93	–140.70	–119.84
Co^{2+}	–107.62	–94.04	–143.26	–115.29	–157.05	–124.49
Ni^{2+}	–116.03	–99.45	–160.20	–126.62	–175.85	–136.93
Cu^{2+}	–135.61	–107.88	–194.74	–146.36	–212.64	–158.25
Zn^{2+}	–104.08	–98.03	–140.46	–127.77	–158.69	–141.37

systems, we have a stabilization of 13.67 kcal/mol from B3LYP and 9.59 kcal/mol from MP2 for Co^{2+} binding H_2Se_2 with respect to the H_2S_2 binding.

MP2 could provide a better description of electronic structure,[66,67] while the use of a large basis set can decrease differences[68,69] that however can be found to be even larger in some cases,[70,71] but recent calculations on transition metals have found a similar kind of differences with respect to DFT, sometimes finding that DFT calculations provide the correct results[72,73] when MP2 fails since the perturbation procedure is performed on a wrong initial determinant. Since experiments directly comparable with our calculations are not available, it is difficult to say which method provides the most reliable results. To check reliability of MP2 calculations, we investigated the stability of the obtained wave functions, finding that all the wavefuntions are stable. Thus, we performed an investigation of MP convergence, doing perturbation calculations up to fourth order. In Figure 4 we report the correction energy for MP2, MP3, and MP4 for H_2O_2 and H_2S_2 binding to metals. The convergence is not totally achieved since MP4 corrections are larger than MP3 ones, but both are smaller than MP2 correc-

TABLE 4: Binding Free Energy (ΔG, in kcal/mol) Calculated at the B3LYP and MP2 Levels

	H_2O_2		H_2S_2		H_2Se_2	
	B3LYP	MP2	B3LYP	MP2	B3LYP	MP2
Mn^{2+}	–79.62	–71.03	–97.96	–81.06	–109.72	–89.52
Fe^{2+}	–92.09	–80.29	–119.30	–96.32	–132.04	–110.10
Co^{2+}	–99.56	–86.00	–134.52	–106.14	–148.19	–115.73
Ni^{2+}	–108.02	–91.36	–151.51	–117.72	–167.04	–128.01
Cu^{2+}	–128.40	–99.83	–186.31	–136.74	–204.39	–148.98
Zn^{2+}	–96.36	–90.30	–131.97	–119.26	–150.02	–132.78

tions, and thus, a strong criticism to MP2 results is not honestly fully possible from these results as was, on the contrary, possible for Cu^+.[72]

We thus performed single-point CCSD(T) calculations on both MP2- and B3LYP-optimized structures, and binding energies (ΔE) are reported for all complexes in Table 5. Further, we tested the performance of other popular functionals: MPW1PW91, M05, TPSS, BLYP, and SVWN. We chose these functionals among the huge number of existing functionals since they are currently employed in common DFT codes. BLYP is a typically used functional where both exchange[54] and correlation[55] are treated via DFT, and since it has a relatively low computational cost, it is currently employed for large systems and DFT-based molecular dynamics.[74] MPW1PW91 is a one-parameter hybrid functional which uses modified Perdew−Wang exchange and Perdew−Wang 91 correlation.[1] M05 belongs the class of newly developed functionals based on hybrid-meta-DFT that are reported to provide better results with respect to common hybrid-DFT.[45,46] TPSS is a meta-DFT functional that can be useful in comparison with meta-hybrid-DFT to understand the importance of Hartree−Fock exchange. Finally, the SVWN functional, which is based on the electron gas uniform density approximation, uses Slater exchange[56] and the VWN correlation functional,[57] and sometimes it can provide good results, as was shown in the case of extended conjugated systems.[75] As clearly shown from Table 4, MP2 provides binding energies closer to CCSD(T) values, while DFT always overestimates binding energy. The MPW1PW91 functional provides the better results among the tested functionals, better than M05 and B3LYP. The other functionals, on the other hand, report binding energies that are even more overestimated with respect to CCSD(T) values. Note that CCSD(T) reports the same metal binding energy affinity for all complexes ($Cu^{2+} > Ni^{2+} > Zn^{2+} > Co^{2+} > Fe^{2+} > Mn^{2+}$), thus simplifying the pictures emerged from MP2 and DFT calculations where some binding energies between different metals were too similar, clearly within the method's error bar, and the order is not the same for all chalcogens.

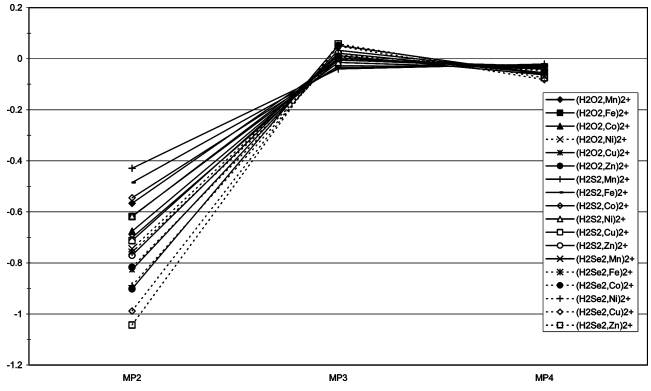

Figure 4. Values of the electron correlation energy (in hartrees) up to the fourth order.

In the same table, Table 5, we also report the mean absolute distance (often called the mean unsigned error) where we use CCSD(T) results as a reference. In this way it is possible to summarize the performance of different methods. Note that systematically H_2O_2 complexes are described better than H_2S_2 and H_2Se_2. Globally MP2 provides binding energies very close to CCSD(T) ones, hybrid functionals present errors of about 10−20 kcal/mol, and other functionals totally fail. In particular, we should mention that Mn^{2+} and Zn^{2+} are metals whose binding energies to the three complexes are better evaluated, with respect to CCSD(T) reference values, from all the methods here employed.

As we previously remarked, MP2 and B3LYP calculations provide different interaction energies, in particular B3LYP systematically overestimates $M^{2+}-H_2X_2$ binding, with corresponding different electronic structure description and wave function character, in particular when the interaction energy is stronger. The same overbinding was found by other functionals such that we can argue that this is a common DFT feature. Thus, CCSD(T) calculations were employed to understand which method mainly fails. MP2 seems to work better for these complexes. In fact, even if some discrepancies are found they are smaller than those obtained from B3LYP calculations, and in some cases (e.g., Zn^{2+} complexes), the agreement between MP2 and CCSD(T) is very good.

In the following we will discuss results obtained with both B3LYP and MP2 methods to identify the electronic structure failures that should be at the origin of the large difference between B3LYP and MP2 results. We should remember that MP2 provides the better agreement with CCSD(T) calculations that can be considered as a reference. Note that even if the global picture concerning binding energies behavior across the series is not qualitatively modified, the absolute values of binding energies are largely different (and the difference increases as the binding affinity increases), and as we will discuss in what follows, this reflects strong differences in the electronic structure of the complexes.

3.3. Electronic Structure. NBO analysis was systematically performed on all complexes optimized structures in order to understand differences in structure and binding energies as a function of both the chalcogen and the transition metal. We report charges and spin densities found on all atoms in Tables 6 and 7, respectively. We note that moving from Mn to Cu the metal charge, being formally +2, drops down and goes back up for Zn. It should also be noted that B3LYP calculations provide a systematically smaller charge on the metal with respect to MP2 results: such complexes present a higher molecule-to-metal electron transfer character, thus explaining the larger stabilization reported by B3LYP. This discrepancy between B3LYP and MP2 charges is due to a too high ligand-to-metal electron transfer, so that these B3LYP charges cannot be used even for a qualitative understanding.

Changing the nature of the chalcogen, the metal charge gets smaller moving from O to S and from S to Se. Spin density also reflects this behavior. We thus investigated through NBO analysis the nature of interactions. In Table 8 we report chemical bonds as found by NBO analysis. Note that for all complexes, except the $[Zn(H_2X_2)]^{2+}$ system, we have open shell systems. Thus, we can distinguish between α and β electrons shared by two atoms such that a 2-electron chemical bond is formed by one α and one β electron for HX and XX bonds, marked with α/β label in the table. Further, we found some X−M bonds

TABLE 5: Binding Energies (in kcal/mol) Calculated at CCSD(T) (using both MP2- and B3LYP-optimized geometries), MP2, B3LYP, MPW1PW91, M05, TPSS, BLYP, and SVWN[a]

	CCSD(T)								
	geometry MP2	geometry B3LYP	MP2	B3LYP	MPW1PW91	M05	TPSS	BLYP	SVWN
$(MnH_2O_2)^{2+}$	–79.56	–79.40	–78.77	–87.40	–85.28	–83.68	–91.84	–92.63	–108.35
$(FeH_2O_2)^{2+}$	–89.93	–89.75	–88.50	–99.57	–96.72	–96.87	–106.14	–107.88	–126.00
$(CoH_2O_2)^{2+}$	–96.14	–95.87	–94.04	–107.62	–104.52	–106.56	–115.39	–118.87	–141.31
$(NiH_2O_2)^{2+}$	–102.32	–101.82	–99.45	–116.03	–112.03	–113.74	–126.38	–130.55	–155.64
$(CuH_2O_2)^{2+}$	–113.98	–111.54	–107.88	–135.61	–129.31	–132.42	–149.09	–154.60	–177.78
$(ZnH_2O_2)^{2+}$	–97.81	–97.77	–98.03	–104.08	–101.46	–98.01	–106.89	–109.21	–123.94
$MAD(MH_2O_2)^{2+}$	0	0.60	2.25	11.76	8.26	8.59	19.33	22.33	42.21
$(MnH_2S_2)^{2+}$	–92.15	–92.11	–89.73	–106.82	–104.03	–103.07	–113.75	–117.46	–134.76
$(FeH_2S_2)^{2+}$	–109.39	–109.23	–104.93	–127.80	–123.73	–125.50	–137.18	–142.26	–163.72
$(CoH_2S_2)^{2+}$	–121.69	–121.50	–115.29	–143.26	–138.46	–137.89	–152.74	–161.07	–186.92
$(NiH_2S_2)^{2+}$	–136.45	–136.10	–126.62	–160.20	–154.36	–162.81	–171.37	–180.09	
$(CuH_2S_2)^{2+}$	–166.64	–168.36	–146.36	–194.74	–187.22	–195.19	–205.21	–214.59	–241.57
$(ZnH_2S_2)^{2+}$	–127.46	–127.51	–127.77	–140.46	–136.37	–134.36	–142.41	–149.96	–165.52
$MAD(MH_2S_2)^{2+}$	0	0.42	7.28	19.92	15.07	17.51	28.15	35.28	55.03
$(MnH_2Se_2)^{2+}$	–100.67	–100.68	–97.86	–118.35	–115.24	–116.28	–125.91	–130.31	–146.56
$(FeH_2Se_2)^{2+}$	–119.04	–119.13	–119.84	–140.70	–136.00	–141.11	–150.86	–156.18	
$(CoH_2Se_2)^{2+}$	–131.82	–131.68	–124.49	–157.05	–151.56	–165.09	–166.94	–176.38	–200.58
$(NiH_2Se_2)^{2+}$	–148.48	–148.21	–136.93	–175.85	–169.31	–182.98	–187.47	–197.30	
$(CuH_2Se_2)^{2+}$	–181.25	–189.74	–158.25	–212.64	–204.69	–219.24	–223.26	–233.55	–259.09
$(ZnH_2Se_2)^{2+}$	–141.39	–141.53	–141.37	–158.69	–153.80	–154.12	–160.80	–169.80	–184.02
$MAD(MH_2Se_2)^{2+}$	0	1.52	7.59	23.44	17.99	26.03	32.10	40.15	58.78
MAD/Tot	0	0.85	5.71	18.37	13.77	17.38	26.52	35.59	52.01

[a] MAD is the mean absolute distance, where as reference we used CCSD(T) calculations done with MP2-optimized geometries.

TABLE 6: Charges of Optimized Structures Calculated at Both the MP2 and B3LYP Levels

	q(H)		*q*(O)		*q*(M)	
	B3LYP	MP2	B3LYP	MP2	B3LYP	MP2
H_2O_2	+0.454	+0.460	–0.454	–0.460		
$(MnH_2O_2)^{2+}$	+0.569	+0.571	–0.489	–0.543	+1.840	+1.944
$(FeH_2O_2)^{2+}$	+0.576	+0.578	–0.464	–0.543	+1.776	+1.929
$(CoH_2O_2)^{2+}$	+0.576	+0.580	–0.437	–0.539	+1.722	+1.919
$(NiH_2O_2)^{2+}$	+0.579	+0.583	–0.408	–0.539	+1.658	+1.911
$(CuH_2O_2)^{2+}$	+0.580	+0.588	–0.301	–0.535	+1.442	+1.894
$(ZnH_2O_2)^{2+}$	+0.576	+0.584	–0.501	–0.551	+1.850	+1.936
H_2S_2	+0.117	+0.098	–0.117	–0.098		
$(MnH_2S_2)^{2+}$	+0.226	+0.205	–0.005	–0.101	+1.559	+1.791
$(FeH_2S_2)^{2+}$	+0.226	+0.207	+0.063	–0.081	+1.422	+1.750
$(CoH_2S_2)^{2+}$	+0.226	+0.209	+0.111	–0.073	+1.326	+1.728
$(NiH_2S_2)^{2+}$	+0.226	+0.210	+0.149	–0.059	+1.249	+1.699
$(CuH_2S_2)^{2+}$	+0.226	+0.214	+0.242	–0.025	+1.064	+1.622
$(ZnH_2S_2)^{2+}$	+0.228	+0.208	+0.015	–0.065	+1.515	+1.714
H_2Se_2	+0.070	+0.044	–0.070	–0.044		
$(MnH_2Se_2)^{2+}$	+0.165	+0.135	+0.090	–0.012	+1.490	+1.754
$(FeH_2Se_2)^{2+}$	+0.167	+0.139	+0.162	–0.011	+1.343	+1.701
$(CoH_2Se_2)^{2+}$	+0.167	+0.140	+0.213	+0.020	+1.240	+1.680
$(NiH_2Se_2)^{2+}$	+0.167	+0.141	+0.252	+0.037	+1.163	+1.644
$(CuH_2Se_2)^{2+}$	+0.167	+0.148	+0.337	+0.074	+0.992	+1.556
$(ZnH_2Se_2)^{2+}$	+0.165	+0.139	+0.136	+0.041	+1.397	+1.641

composed of one unpaired electron, marked with β in the same table, where for convention sake we assign the unpaired electron to β spin.

Looking carefully for bonding analysis reported in Table 8, we should first note that H_2O_2 does not form any bond with any metals for the MP2 wave function, while the B3LYP wave function presents an O−M bond for each O atom mixing p orbitals of O with hybrid sd orbitals of the metal for Ni^{2+}, while for Cu^{2+} we found only one O−Cu bond mixing p orbitals of O with d orbitals of Cu. This is quite expected since Cu^{2+} has a d^9 electronic configuration, and thus, only one orbital can be shared with O atoms. However, this can be also an artifact in DFT calculations due to a wrong position of the atomic orbital levels of Cu^{2+}. It is also the most stable structure, more stable than those forming two bonds, which can be apparently in contradiction with this last property. The larger O−Cu distance in the series is coherent with this trend in chemical bonds. The stabilization is thus mainly due to the bigger charge transfer, as reported by both lower charge on Cu, 1.44 for B3LYP and 1.89 for MP2. As we will see, this charge transfer is even much important for stabilization of $[Cu(H_2S_2)]^{2+}$ and $[Cu(H_2Se_2)]^{2+}$ complexes.

H_2S_2 and H_2Se_2 complexes show a similar behavior in bond formation. Moving across the transition metal series, MP2 found a bond between Ni^{2+} and Se, still composed by p orbitals of the chalcogen and hybrid sd orbitals of the metal and the same kind of bond thus for H_2S_2 and H_2Se_2 binding with Cu^{2+}. Zn^{2+}, which has d orbitals fully occupied, forms, on the other hand, a bond involving p orbitals of S or Se and hybrid sp orbitals of the metal.

B3LYP provides the formation of bonds between Mn^{2+}, Fe^{2+}, and Co^{2+} and S or Se and between Ni^{2+} and S that are not

TABLE 7: Spin Densities (*s*) of Optimized Structures Calculated at Both the MP2 and B3LYP Levels

	s(H)		*s*(X)		*s*(M)	
	B3LYP	MP2	B3LYP	MP2	B3LYP	MP2
$(MnH_2O_2)^{2+}$	0.0067	0.0027	0.0411	0.0024	4.9044	4.9899
$(FeH_2O_2)^{2+}$	0.0064	0.0027	0.0722	0.0100	3.8427	3.9746
$(CoH_2O_2)^{2+}$	0.0041	0.0011	0.1017	0.0168	2.7886	2.9641
$(NiH_2O_2)^{2+}$	0.0026	0.0027	0.1376	0.0218	1.7198	1.9559
$(CuH_2O_2)^{2+}$	0.0012	0.0001	0.2631	0.0316	1.4422	0.9367
$(MnH_2S_2)^{2+}$	0.0053	0.0027	0.0961	–0.0045	4.7973	5.0034
$(FeH_2S_2)^{2+}$	0.0016	–0.0014	0.1739	0.0154	3.6489	3.9719
$(CoH_2S_2)^{2+}$	–0.0016	–0.0020	0.2307	0.0328	2.5417	2.9385
$(NiH_2S_2)^{2+}$	–0.0041	–0.0047	0.2822	0.0509	1.4439	1.9075
$(CuH_2S_2)^{2+}$	–0.0052	–0.0061	0.4053	0.0962	0.1999	0.8197
$(MnH_2Se_2)^{2+}$	0.0054	0.0030	0.0833	–0.0230	4.8225	5.0401
$(FeH_2Se_2)^{2+}$	0.0009	–0.0020	0.1748	0.0001	3.6485	4.0038
$(CoH_2Se_2)^{2+}$	–0.0036	–0.0019	0.2422	0.0193	2.5229	2.9653
$(NiH_2Se_2)^{2+}$	–0.0074	–0.0053	0.3003	0.0448	1.4143	1.9211
$(CuH_2Se_2)^{2+}$	–0.0082	–0.0065	0.4206	0.1042	0.1752	0.8046

TABLE 8: NBO Analysis: Bonds Obtained from B3LYP and MP2 Wavefunctions[a]

	H_2O_2		H_2S_2		H_2Se_2	
	B3LYP	MP2	B3LYP	MP2	B3LYP	MP2
Mn^{2+}	H^1-O^2 (α/β) H^4-O^3 (α/β) O^2-O^3 (α/β)	H^1-O^2 (α/β) H^4-O^3 (α/β) O^2-O^3 (α/β)	H^1-S^2 (α/β) H^4-S^3 (α/β) S^2-S^3 (α/β) S^2-Mn (β) S^3-Mn (β)	H^1-S^2 (α/β) H^4-S^3 (α/β) S^2-S^3 (α/β)	H^1-Se^2 (α/β) H^4-Se^3 (α/β) Se^2-Se^3 (α/β) Se^2-Mn (β) Se^3-Mn (β)	H^1-Se^2 (α/β) H^4-Se^3 (α/β) Se^2-Se^3 (α/β)
Fe^{2+}	H^1-O^2 (α/β) H^4-O^3 (α/β) O^2-O^3 (α/β)	H^1-O^2 (α/β) H^4-O^3 (α/β) O^2-O^3 (α/β)	H^1-S^2 (α/β) H^4-S^3 (α/β) S^2-S^3 (α/β) S^2-Fe (β) S^3-Fe (β)	H^1-S^2 (α/β) H^4-S^3 (α/β) S^2-S^3 (α/β)	H^1-Se^2 (α/β) H^4-Se^3 (α/β) Se^2-Se^3 (α/β) Se^2-Fe (β) Se^3-Fe (β)	H^1-Se^2 (α/β) H^4-Se^3 (α/β) Se^2-Se^3 (α/β)
Co^{2+}	H^1-O^2 (α/β) H^4-O^3 (α/β) O^2-O^3 (α/β)	H^1-O^2 (α/β) H^4-O^3 (α/β) O^2-O^3 (α/β)	H^1-S^2 (α/β) H^4-S^3 (α/β) S^2-S^3 (α/β) S^2-Co (β) S^3-Co (β)	H^1-S^2 (α/β) H^4-S^3 (α/β) S^2-S^3 (α/β)	H^1-Se^2 (α/β) H^4-Se^3 (α/β) Se^2-Se^3 (α/β) Se^2-Co (β) Se^3-Co (β)	H^1-Se^2 (α/β) H^4-Se^3 (α/β) Se^2-Se^3 (α/β)
Ni^{2+}	H^1-O^2 (α/β) H^4-O^3 (α/β) O^2-O^3 (α/β) O^2-Ni (β) O^3-Ni (β)	H^1-O^2 (α/β) H^4-O^3 (α/β) O^2-O^3 (α/β)	H^1-S^2 (α/β) H^4-S^3 (α/β) S^2-S^3 (α/β) S^2-Ni (β) S^3-Ni (β)	H^1-S^2 (α/β) H^4-S^3 (α/β) S^2-S^3 (α/β)	H^1-Se^2 (α/β) H^4-Se^3 (α/β) Se^2-Se^3 (α/β) Se^2-Ni (β) Se^3-Ni (β)	H^1-Se^2 (α/β) H^4-Se^3 (α/β) Se^2-Se^3 (α/β) Se^2-Ni (β) Se^3-Ni (β)
Cu^{2+}	H^1-O^2 (α/β) H^4-O^3 (α/β) O^2-O^3 (α/β) O^2-Cu (β)	H^1-O^2 (α/β) H^4-O^3 (α/β) O^2-O^3 (α/β)	H^1-S^2 (α/β) H^4-S^3 (α/β) S^2-S^3 (α/β) S^2-S^3 (β)	H^1-S^2 (α/β) H^4-S^3 (α/β) S^2-S^3 (α/β) S^2-Cu (β) S^3-Cu (β)	H^1-Se^2 (α/β) H^4-Se^3 (α/β) Se^2-Se^3 (α/β) Se^2-Se^3 (β)	H^1-Se^2 (α/β) H^4-Se^3 (α/β) Se^2-Se^3 (α/β) Se^2-Cu (β) Se^3-Cu (β)
Zn^{2+}	H^1-O^2 H^4-O^3 O^2-O^3	H^1-O^2 H^4-O^3 O^2-O^3	H^1-S^2 H^4-S^3 S^2-S^3 S^2-Zn S^3-Zn	H^1-S^2 H^4-S^3 S^2-S^3 S^2-Zn S^3-Zn	H^1-Se^2 H^4-Se^3 Se^2-Se^3 Se^2-Zn Se^3-Zn	H^1-Se^2 H^4-Se^3 Se^2-Se^3 Se^2-Zn Se^3-Zn

[a] Atoms of H_2X_2 molecules are numbered as $H^1-X^2-X^3-H^4$.

found by MP2, notably a bond between p orbitals of two chalcogens and a hybrid sd orbital of the metal, while only the $Ni^{2+}-Se$ bond was found by both B3LYP and MP2. For Cu^{2+} the picture is different: no electron was found to be in common between S or Se and the metal, but an electron transfer was observed, from B3LYP calculations, such that Cu^{2+} is reduced to Cu^+ by an electron donated by the S or Se lone pairs. Thus, now the two chalcogens can form an additional one-electron bond that is found only for $[Cu(H_2S_2)]^{2+}$ and $[Cu(H_2Se_2)]^{2+}$ complexes with the B3LYP wave function. This explains the bigger Cu−X distance found in B3LYP geometries and the consequent shortening of S−S and Se−Se bond, such that the overall complex is now more stable. This is more clearly shown in Table 9, where we show the projection of the wave function on the atomic orbitals of the metals. In particular, we should note that, up to B3LYP calculations, 3d orbitals of Cu

TABLE 9: Occupancy of 5d Atomic Orbitals of the Transition Metals by Wave Function Projection[a]

	H_2O_2		H_2S_2		H_2Se_2	
	B3LYP	MP2	B3LYP	MP2	B3LYP	MP2
Mn^{2+}	5.09	5.02	5.23	5.05	5.24	5.05
Fe^{2+}	6.15	6.02	6.37	6.06	6.39	6.07
Co^{2+}	7.20	7.03	7.47	7.07	7.51	7.07
Ni^{2+}	8.26	8.03	8.55	8.08	8.60	8.08
Cu^{2+}	9.49	9.04	9.77	9.14	9.81	9.15
Zn^{2+}	9.99	10.0	9.99	10.0	9.99	10.0

[a] B3LYP and MP2 results are reported.

are almost fulfilled by one electron coming from hybrid sp orbitals of S and Se. One lone pair has now basically lost one electron, and the remaining electron is shared between the two chalcogens, forming the one-electron bond noted previously. These additional S−S and Se−Se bonds are responsible for the smaller bond distance. It should be noted that this behavior was pointed out only from B3LYP calculations. MP2 did not find such a relevant charge transfer but the formation of bonds between Cu and the two chalcogen atoms, such that the M−X distance is shorter following the binding strength trend across the series. For the sake of completeness, we should note that even if the electron transfer from the molecule to Cu(II) is not so large, the S−S and Se−Se distances are also shortened when forming complexes with Cu^{2+}, probably because the phenomenon so largely noticed from B3LYP calculations, i.e., charge transfer and formation of an additional X−X bond, here has only a small intensity in MP2 wave functions. For Zn^{2+} complexes, we found the same kind of bonds and similar electronic structure from both MP2 and B3LYP calculations. Thus, from results presented in Table 8, it seems that DFT fails in NBO analysis in the unrestricted formalism because no strong difference can be pointed out for Zn^{2+} complexes.

Before concluding, we pause to understand why B3LYP and DFT, in general, provides binding energies largely different with respect to CCSD(T). A possible problem can reside in the multiconfigurational character of the $(MH_2X_2)^{2+}$ wave function. Coupled cluster amplitudes can shed some light on that problem. The largest coupled clusters amplitudes for all the system studied are reported in the Supporting Information. These amplitudes are quite large for systems containing Cu^{2+}, and they become larger with the increase of the chalcogen atomic number. The big discrepancy found for Cu^{2+} systems can be explained with a shortfall in describing a wave function with an intrinsic multiconfigurational character. Cu^{2+}-containing systems seem to be the most problematic ones, where the wave function has the largest multiconfigurational character and where B3LYP found that the metal is in the Cu^{+} oxidation state. In other words, the wave function can have a double character, Cu^{+}/X^{+} and Cu^{2+}/X, reflecting the fact that Cu has the highest second ionization energy. CCSD(T) calculations provide a second ionization potential of 465.55 kcal/mol, while B3LYP and MP2 have 480.34 and 483.33 kcal/mol, respectively. Thus, as reflected by partial charges on Cu, the Cu^{+}/X^{+} character is overestimated by B3LYP. When forming the complexes, B3LYP and DFT, in general, do not correctly describe a static correlation that can give the correct weights between the two characters, and thus, the binding energy is largerly different from CCSD(T) results. In MP2 calculations there is an overestimation of static correlation and then in some case, like for $(CuH_2O_2)^{2+}$, it can be an error compensation effect. For Zn, Ni, and Co, on the other hand, second ionization potentials obtained from MP2 (403.72, 423.12, and 391.52 kcal/mol, respectively) are more similar to CCSD(T) results (402.88, 410.55, and 384.11 kcal/mol, respectively) than B3LYP ones (423.87, 432.35, and 409.51 kcal/mol) such that across the series MP2 results are, on average, better than B3LYP ones.

4. Conclusions and Outlook

In this paper we investigated the binding properties of divalent first row transition metals from Mn^{2+} to Zn^{2+} with minimal molecular models of chalcogen−chalcogen bridges, H_2O_2, H_2S_2, and H_2Se_2. The DFT and MP2 level of theory are compared, and using CCSD(T) data as references, we found that DFT has severe problems, while MP2 data match more closely with those reference calculations. Even if DFT can come to similar qualitative conclusions, the discrepancy with MP2 can be large. In particular, the description of Cu^{2+} binding to H_2X_2 seems to be a problem for DFT, and this is noticed in terms of binding energies, metal−chalcogen distances, and electronic structures. More, in general, DFT tends to overestimate metal/complex binding energy, mainly because it overestimates a molecule-to-metal charge transfer that overstabilizes the resulting complexes.

On the basis of MP2 calculations, we found a global trend through the transition metal first row series such that we have a decrease in M−X distances from Mn^{2+} to Cu^{2+} and then a bigger one for Zn^{2+}. Binding energy behavior across the series also follows this trend. Moreover, for each given transition metal, the binding energy trend is $H_2Se_2 > H_2S_2 > H_2O_2$, where the biggest energy difference is between H_2S_2 and H_2O_2.

The binding energy order, from CCSD(T) calculations, was found to be $Cu^{2+} > Ni^{2+} > Zn^{2+} > Co^{2+} > Fe^{2+} > Mn^{2+}$, while MP2 calculations found Ni^{2+} and Zn^{2+} positions inverted even if with similar energies.

This failure of DFT calculations using standard functionals could be surprising, but it can give us a guide when their use is compulsory in calculations involving transition metal binding biological motifs. In particular, great attention must be paid when using GGA DFT functionals like BLYP, as currently done in DFT-based molecular dynamics, such as the Car−Parrinello method that takes many crucial advantages in using DFT to obtain the potential energy surface on the fly.[74] Two ways could be employed to overcome DFT limits and must be adopted when treating systems similar to those presented in this work: (i) modifying the functional and (ii) modifying the electronic wave function representation using new generation pseudo potentials.[76] The first solution is in line with recent progress by the Truhlar group leading to new generation functionals[45,46] even if the hybrid-meta-GGA M05 functional is not able to provide the correct picture when lacking in static correlation is important (as, in particular, for Cu^{2+}), while it gives better results when the monodeterminant description is correct (as for Zn^{2+}). The new M06 class can probably provide better results even if this kind of system, where the wave function has a so important multideterminant character, can be a difficult task for DFT in general. Another possibility could be using the DFT+U method,[77,78] which emphasizes the role of on-site screened Coulomb interactions, providing a correct description of some transition metal oxide crystals where DFT fails.[79,80] The second one is more connected with Car−Parrinello molecular dynamics, but developing new pseudo potentials specifically done to overcome the failures of DFT should be extended to transition metals to have a more complete picture of the limits of this new intriguing approach.

As shown by coupled cluster amplitudes, the main problematic point seems to be the use of a monodeterminant description. Multiconfigurational calculations are beyond the aim of the present study, but they can be of great interest, in particular, to see if new generation DFT functionals can reproduce properties of systems with an intrinsically multideterminant character.

Finally, we were able to draw some general conclusions on metal binding to chalcogen−chalcogen bridges. In particular, we found that there is a clear preference of binding Cu^{2+} for all the chalcogen−chalcogen bridges, and then Zn^{2+} and Ni^{2+} are the most favored metals. We should notice that Zn and Cu are metals largely abundant in biosystems, where they have a structural role[81] and are involved in several redox reactions.[82,83] Furthermore, the Se−Se bridges seem to bind metals more strongly than S−S, larger than that found for cysteine and

seleno-cysteine only with Co^{2+}, thus providing a possible reason of why selenoproteins have often different biochemical behavior. In particular, it can effect catalytic cycles that are coupled to metal binding, such as that of GPx,[84] enhancing the binding affinity and disadvantaging the metal releasing. Thus, the present study can also provide a guide for interpreting the experimental observation of metal binding where it is not always evident if the molecules with more than one S and/or Se to which the metal is bound are in the reduced or oxided state. In particular, our results suggest, coupled with our previous insights limited on Co(II),[32] that the affinity to Se-substituted biomolecules is stronger with respect to natural sulfur biomolecules when the chalcogen forms an X−X bridge, thus being in the oxided state.

Acknowledgment. We thank Professors M.-P. Gaigeot, M.Yanez, and B. Lévy for fruitful discussions.

Supporting Information Available: Full binding energy information table, with ΔE + ZPE and ΔH, the geometries of all optimized structures in *xyz* format, and the largest couple cluster amplitudes. This material is available free of charge via the Internet at http://pubs.acs.org.

References and Notes

(1) Glusker, J. P. *Adv. Protein Chem.* **1991**, *42*, 1.
(2) Rulisek, L.; Vondrasek, J. *J. Inorg. Biochem.* **1998**, *71*, 115.
(3) Rodgers, M. T.; Armentrout, P. B. *Acc. Chem. Res.* **2004**, *37*, 989.
(4) Ho, P.; Loo, J. A. *J. Am. Chem. Soc.* **1995**, *117*, 11314.
(5) Rogalewicz, F.; Hoppilliard, Y.; Ohanessian, G. *Int. J. Mass Spectrom.* **2000**, *201*, 307.
(6) Strittmatter, E. F.; Lemoff, A. S.; Williams, E. R. *J. Phys. Chem. A* **2000**, *104*, 9793.
(7) Belcastro, M.; Marino, T.; Russo, N.; Toscano, M. *J. Mass Spectrom.* **2005**, *40*, 300.
(8) Friesner, R. A.; Beachy, M. D. *Curr. Opin. Struct. Biol.* **1998**, *8*, 257.
(9) Nakajima, A.; Horikoshi, T.; Sakaguchi, T. *Appl. Microbiol. Biotechnol.* **1981**, *12*, 76.
(10) Landis, G. W.; Yu, M. *Introduction to Environmental Toxicology*, 2nd ed.; CRC Press: Boca Raton, FL, 1999.
(11) Ochiai-I, J. E. *J. Chem. Educ.* **1978**, *55*, 631.
(12) Yocum, C. F.; Pecoraro, V. L. *Curr. Opin. Chem. Biol.* **1999**, *3*, 182.
(13) Woo, E.-J.; Dunwell, J. M.; Goodenough, P. W.; Marvier, A. C.; Pickersgill, R. W. *Nat. Struct. Biol.* **2000**, *7*, 1036.
(14) Sayre, L. M.; Perry, G.; Smith, M. A. *Curr. Opin. Chem. Biol.* **1999**, *3*, 220.
(15) Andreson, A. B.; Hong, S. Y.; Smialek, J. L. *J. Phys. Chem.* **1987**, *91*, 4250.
(16) Duvail, M.; Spezia, R.; Vitorge, P. *ChemPhysChem* **2008**, *9*, 693.
(17) Bridgeman, A. J.; Rothery, J. *J. Chem. Soc., Dalton Trans.* **2000**, *2*, 211.
(18) Trzaskowski, B.; Les, A.; Adamowicz, L.; Deymier, P. A.; Guzman, R.; Stepanian, S. G. *J. Comput. Theor. Nanosci.* **2005**, *2*, 1.
(19) Trzaskowski, B.; Stepanian, S.; Les, A.; Deymier, P. A.; Guzman, R. *J. Comput. Theor. Nanosci.* **2006**, *3*, 1.
(20) Mathe, C.; Mattioli, T. A.; Horner, O.; Lombard, M.; Latour, J. M.; Fontecave, M.; Niviere, V. *J. Am. Chem. Soc.* **2002**, *124*, 4966.
(21) Miyanaga, A.; Fushinobu, S.; Ito, K.; Wakagi, T. *Biochem. Biophys. Res. Commun.* **2001**, *288*, 1169.
(22) Endo, I.; Nojiri, M.; Tsujimura, M.; Nakasako, M.; Yohda, M.; Odaka, M. *J. Inorg. Biochem.* **2001**, *83*, 247.
(23) Meinnel, T.; Blanquet, S.; Dardel, F. *J. Mol. Biol.* **1996**, *262*, 375.
(24) Maret, W.; Vallee, B. L. *Proc. Natl. Acad. Sci. U.S.A.* **1998**, *95*, 3478.
(25) Jacob, C.; Giles, G. I.; Giles, N. M.; Sies, H. *Angew. Chem., Int. Ed.* **2003**, *42*, 4742.
(26) Chen, J.; Berry, M. J. *J. Neurochem.* **2003**, *86*, 1.
(27) Behne, D.; Kyriakopoulos, A. *Annu. Rev. Nutr.* **2001**, *21*, 453.
(28) Schomburg, L.; Schweizer, U.; Holtmann, B.; Flohe, L.; Sendtner, M.; Kohrle, J. *Biochem. J.* **2003**, *370*, 397.
(29) Hill, K. E.; Zhou, J.; McMahan, W. J.; Motley, A. K.; Atkins, J. F.; Gesteland, R. F.; Burk, R. F. *J. Biol. Chem.* **2003**, *278*, 13640.
(30) Goyer, R. A. *Annu. Rev. Nutr.* **2001**, *21*, 453.
(31) Othman, A. I.; El Missiry, M. A. *J. Biochem. Mol. Toxicol.* **1998**, *12*, 345.
(32) Spezia, R.; Tournois, G.; Cartailler, T.; Tortajada, J.; Jeanvoine, Y. *J. Phys. Chem. A* **2006**, *110*, 9727.
(33) Becke, A. D. *J. Chem. Phys.* **1993**, *98*, 5648.
(34) Niu, S.; Hall, M. B. *Chem. Rev.* **2000**, *100*, 353.
(35) Harrison, J. F. *Chem. Rev.* **2000**, *100*, 679.
(36) Baker, J.; Pulay, P. *J. Comput. Chem.* **2003**, *10*, 1184.
(37) Izgorodina, E. I.; Coote, M. L.; Radom, L. *J. Phys. Chem. A* **2005**, *109*, 7558.
(38) Reiher, M.; Salomon, O.; Hess, B. A. *Theor. Chem. Acc.* **2001**, *107*, 48.
(39) Schultz, N.; Zhao, Y.; Truhlar, D. G. *J. Phys. Chem. A* **2005**, *109*, 4388.
(40) Schultz, N.; Zhao, Y.; Truhlar, D. G. *J. Phys. Chem. A* **2005**, *109*, 11127.
(41) Harvey, J. N. *Annu. Rep. Prog. Chem., Sect. C* **2006**, *102*, 203.
(42) Tsipis, A. C.; Orpen, A. G.; Harvey, J. N. *Dalton Trans.* **2005**, 2849.
(43) Zhao, Y.; Truhlar, D. G. *Org. Lett.* **2007**, *9*, 1967.
(44) Poater, J.; Solà, M.; Rimola, A.; Rodriguez-Sanitago, L.; Sodupe, M. *J. Phys. Chem. A* **2004**, *108*, 6072.
(45) Zhao, Y.; Truhlar, D. G. *Acc. Chem. Res.* **2008**, *41*, 157.
(46) Zhao, Y.; Truhlar, D. G. *Theor. Chem. Acc.* **2008**, *119*, 525.
(47) Ruliek, L.; Havlas, Z. *Int. J. Quantum Chem.* **2002**, *91*, 504.
(48) Belcastro, M.; Marino, T.; Russo, N.; Toscano, M. *J. Mass. Spectrom.* **2005**, *40*, 300.
(49) Compagnon, I.; Tabarin, T.; Antoine, R.; Broyer, M.; Dugourd, P.; Mitric, R.; Petersen, J.; Bonacic-Koutecky, V. *J. Chem. Phys.* **2006**, *125*, 164326.
(50) Adamo, C.; Barone, V. *J. Chem. Phys.* **1998**, *108*, 664.
(51) Zhao, Y.; Schultz, N. E.; Truhlar, D. G. *J. Chem. Theory Comput.* **2006**, *2*, 364.
(52) Tao, J.; Perdew, J. P.; Staroverov, V. N.; Scuseria, G. E. *Phys. Rev. Lett.* **2003**, *91*, 146401.
(53) Becke, A. D. *Phys. Rev. A.* **1988**, *38*, 3098.
(54) Lee, C.; Yang, W.; Parr, R. G. *Phys. Rev. B* **1988**, *37*, 785.
(55) Miehlich, B.; Savin, A.; Stoll, H.; Preuss, H. *Chem. Phys. Lett.* **1989**, *157*, 200.
(56) Slater, J. C. *Quantum Theory of Molecular and Solids*; McGraw-Hill: New York, 1974; Vol. 4 (The Self-Consistent Field for Molecular and Solids).
(57) Vosko, S. H.; Wilk, L.; Nusair, M. *Can. J. Phys.* **1980**, *58*, 1200.
(58) Costantino, E.; Rimola, A.; Rodriguez-Santiago, L.; Sodupe, M. *New J. Chem.* **2005**, *29*, 1585.
(59) Spezia, R.; Tournois, G.; Tortajada, J.; Cartailler, T.; Gaigeot, M.-P. *Phys. Chem. Chem. Phys.* **2006**, *8*, 2040.
(60) Buchmann, W.; Spezia, R.; Tournois, G.; Cartailler, T.; Tortajada, J. *J. Mass Spectrom.* **2007**, *42*, 517.
(61) Boys, S. F.; Bernardi, F. *Mol. Phys.* **1970**, *19*, 553.
(62) McQuarrie, D. A. *Statistical Thermodynamics*; Harper and Row: New York, 1973.
(63) Weinhold, F.; Carpenter, J. E. *The Structure of Small Molecules and Ions*; Plenum: New York, 1988.
(64) Carpenter, J. E.; Weinhold, F. *J. Mol. Struct. (THEOCHEM)* **1988**, *169*, 41.
(65) Frisch, M. J.; Trucks, G. W.; Schlegel, H. B.; Scuseria, G. E.; Robb, M. A.; Cheeseman, J. R.; Montgomery, J. A., Jr.; Vreven, T.; Kudin, K. N.; Burant, J. C.; Millam, J. M.; Iyengar, S. S.; Tomasi, J.; Barone, V.; Mennucci, B.; Cossi, M.; Scalmani, G.; Rega, N.; Petersson, G. A.; Nakatsuji, H.; Hada, M.; Ehara, M.; Toyota, K.; Fukuda, R.; Hasegawa, J.; Ishida, M.; Nakajima, T.; Honda, Y.; Kitao, O.; Nakai, H.; Klene, M.; Li, X.; Knox, J. E.; Hratchian, H. P.; Cross, J. B.; Bakken, V.; Adamo, C.; Jaramillo, J.; Gomperts, R.; Stratmann, R. E.; Yazyev, O.; Austin, A. J.; Cammi, R.; Pomelli, C.; Ochterski, J. W.; Ayala, P. Y.; Morokuma, K.; Voth, G. A.; Salvador, P.; Dannenberg, J. J.; Zakrzewski, V. G.; Dapprich, S.; Daniels, A. D.; Strain, M. C.; Farkas, O.; Malick, D. K.; Rabuck, A. D.; Raghavachari, K.; Foresman, J. B.; Ortiz, J. V.; Cui, Q.; Baboul, A. G.; Clifford, S.; Cioslowski, J.; Stefanov, B. B.; Liu, G.; Liashenko, A.; Piskorz, P.; Komaromi, I.; Martin, R. L.; Fox, D. J.; Keith, T.; Al Laham, M. A.; Peng, C. Y.; Nanayakkara, A.; Challacombe, M.; Gill, P. M. W.; Johnson, B.; Chen, W.; Wong, M. W.; Gonzalez, C.; Pople, J. A. *Gaussian 03*, Revision D.01; Gaussian, Inc.: Wallingford CT, 2004. Revision E.01 was used for M05 and TPSS calculations.
(66) Kieninger, M.; Cachau, R. E.; Oberhammer, H.; Ventura, O. N. *Int. J. Quantum Chem.* **2006**, *107*, 403.
(67) Rubio-Pons, O.; Luo, Y. *J. Chem. Phys.* **2004**, *121*, 157.
(68) Paizs, B.; Suhai, S. *J. Comput. Chem.* **1998**, *19*, 575.
(69) Murashov, V. V.; Leszczynski, J. *J. Mol. Struct. (THEOCHEM)* **2000**, *529*, 1.
(70) Niewodniczanski, W.; Bartowiak, W.; Leszczynski, J. *J. Mol. Model.* **2005**, *11*, 392.
(71) Sekusak, S.; Frenking, G. *J. Mol. Struct. (THEOCHEM)* **2001**, *541*, 17.

(72) Luna, A.; Alcamì, M.; Mo, O.; Yanez, M. *Chem. Phys. Lett.* **2000**, *320*, 129.
(73) Lynch, B. J.; Truhlar, D. G. *Chem. Phys. Lett.* **2002**, *361*, 251.
(74) Car, R.; Parrinello, M. *Phys. Rev. Lett.* **1985**, *55*, 2471.
(75) Spezia, R.; Zazza, C.; Palma, A.; Amadei, A.; Aschi, M. *J. Phys. Chem. A* **2004**, *108*, 6763.
(76) Lin, I.-C.; Coutinho-Neto, M. D.; Felsenheimer, C.; von Lilienfeld, O. A.; Tavernelli, I.; Rothlisberger, U. *Phys. Rev. B* **2007**, *75*, 205131.
(77) Anisimov, V. I.; Zaanen, J.; Andersen, O. K. *Phys. Rev. B* **1991**, *44*, 943.
(78) Liechtenstein, A. I.; Anisimov, A. I.; Zaanen, J. *Phys. Rev. B* **1995**, *52*, 5467.
(79) Nekrasov, I. A.; Streltsov, S. V.; Korotin, M. A.; Anisimov, V. I. *Phys. Rev. B* **2003**, *68*, 235113.
(80) Pickett, W. E.; Erwin, S. C.; Ethridge, E. C. *Phys. Rev. B* **1998**, *58*, 1201.
(81) Christianson, D. W. *Adv. Protein Chem.* **1991**, *42*, 281.
(82) Maret, W.; Vallee, B. L. *Proc. Natl. Acad. Sci.* **1996**, *95*, 3478.
(83) Karlin, K. D. *Science* **1993**, *261*, 701.
(84) Giles, N. M.; Gutowski, N. J.; Giles, G. I.; Jacob, C. *FEBS Lett.* **2003**, *535*, 179.

JP811460F